



AFRL-RY-WP-TP-2013-0021

**WIDELY-TUNABLE PARAMETRIC SHORT-WAVE
INFRARED TRANSMITTER FOR CO₂ TRACE
DETECTION (POSTPRINT)**

Nicholas G. Usechak

**Optoelectronic Technology Branch
Aerospace Components & Subsystems Division**

Slaven Moro, Nikola Alic, and Stojan Radic

University of California

Aleksandar Danicic

Vinča Institute of Nuclear Sciences

JANUARY 2013

Interim

Approved for public release; distribution unlimited.

See additional restrictions described on inside pages

© 2011 Optical Society of America

STINFO COPY

**AIR FORCE RESEARCH LABORATORY
SENSORS DIRECTORATE
WRIGHT-PATTERSON AIR FORCE BASE, OH 45433-7320
AIR FORCE MATERIEL COMMAND
UNITED STATES AIR FORCE**

REPORT DOCUMENTATION PAGE				<i>Form Approved</i> OMB No. 0704-0188	
<p>The public reporting burden for this collection of information is estimated to average 1 hour per response, including the time for reviewing instructions, searching existing data sources, gathering and maintaining the data needed, and completing and reviewing the collection of information. Send comments regarding this burden estimate or any other aspect of this collection of information, including suggestions for reducing this burden, to Department of Defense, Washington Headquarters Services, Directorate for Information Operations and Reports (0704-0188), 1215 Jefferson Davis Highway, Suite 1204, Arlington, VA 22202-4302. Respondents should be aware that notwithstanding any other provision of law, no person shall be subject to any penalty for failing to comply with a collection of information if it does not display a currently valid OMB control number. PLEASE DO NOT RETURN YOUR FORM TO THE ABOVE ADDRESS.</p>					
1. REPORT DATE (DD-MM-YY) January 2013		2. REPORT TYPE Journal Article Postprint		3. DATES COVERED (From - To) 15 September 2008 – 14 April 2011	
4. TITLE AND SUBTITLE WIDELY-TUNABLE PARAMETRIC SHORT-WAVE INFRARED TRANSMITTER FOR CO2 TRACE DETECTION (POSTPRINT)				5a. CONTRACT NUMBER In-house	
				5b. GRANT NUMBER	
				5c. PROGRAM ELEMENT NUMBER 61102F	
6. AUTHOR(S) Nicholas G. Usechak (AFRL/RYPDH) Slaven Moro, Nikola Alic, and Stojan Radic (University of California) Aleksandar Danicic (Vinča Institute of Nuclear Sciences)				5d. PROJECT NUMBER 2305	
				5e. TASK NUMBER DP	
				5f. WORK UNIT NUMBER Y05T	
7. PERFORMING ORGANIZATION NAME(S) AND ADDRESS(ES) Optoelectronic Technology Branch Aerospace Components & Subsystems Division Air Force Research Laboratory, Sensors Directorate Wright-Patterson Air Force Base, OH 45433-7320 Air Force Materiel Command, United States Air Force				8. PERFORMING ORGANIZATION REPORT NUMBER AFRL-RY-WP-TP-2013-0021	
9. SPONSORING/MONITORING AGENCY NAME(S) AND ADDRESS(ES) Air Force Research Laboratory Sensors Directorate Wright-Patterson Air Force Base, OH 45433-7320 Air Force Materiel Command United States Air Force				10. SPONSORING/MONITORING AGENCY ACRONYM(S) AFRL/RYPDH	
				11. SPONSORING/MONITORING AGENCY REPORT NUMBER(S) AFRL-RY-WP-TP-2013-0021	
12. DISTRIBUTION/AVAILABILITY STATEMENT Approved for public release; distribution unlimited.					
13. SUPPLEMENTARY NOTES Journal article published in Optics Express, 25 April 2011. ©2011 Optical Society of America. The U.S. Government is joint author of the work and has the right to use, modify, reproduce, release, perform, display or disclose the work. PAO Case Number 88ABW-2010-6315, Clearance Date 1 December 2010. Report contains color.					
14. ABSTRACT An all-fiber, tunable, short-wave infrared transmitter is demonstrated using efficient four-wave mixing in conventional L and O bands. To realize this source a highly-nonlinear fiber, exhibiting low bend loss over the short-wave infrared spectral band, is employed because of its advantageous properties as a nonlinear mixing medium. The transmitter was subsequently exploited to probe and detect trace levels of carbon dioxide in the 2051-nm spectral region where its beam properties, tunability, narrow linewidth, and stability all coalesce to permit this application. This work indicates this transmitter can serve as a robust source for sensing carbon dioxide and other trace gasses in the short-wave infrared spectral region and should therefore play an important role in future applications.					
15. SUBJECT TERMS Parametric amplifiers and oscillators, nonlinear optics, four-wave mixing, nonlinear fiber optics, SWIR sources, tunable sources					
16. SECURITY CLASSIFICATION OF:			17. LIMITATION OF ABSTRACT: SAR	18. NUMBER OF PAGES 8	19a. NAME OF RESPONSIBLE PERSON (Monitor) Nicholas Usechak
a. REPORT Unclassified	b. ABSTRACT Unclassified	c. THIS PAGE Unclassified			

Widely-tunable parametric short-wave infrared transmitter for CO₂ trace detection

Slaven Moro,^{1,*} Aleksandar Danicic,² Nikola Alic,¹
Nicholas G. Usechak,³ and Stojan Radic¹

¹University of California – San Diego, 9500 Gilman Drive, La Jolla, California 92093, USA

²Vinča Institute of Nuclear Sciences, 11001 Belgrade, Serbia

³Air Force Research Laboratory, 2241 Avionics Circle, Wright-Patterson AFB, Dayton, Ohio, USA

*smoro@ucsd.edu

Abstract: An all-fiber, tunable, short-wave infrared transmitter is demonstrated using efficient four-wave mixing in conventional L and O bands. To realize this source a highly-nonlinear fiber, exhibiting low bend loss over the short-wave infrared spectral band, is employed because of its advantageous properties as a nonlinear mixing medium. The transmitter was subsequently exploited to probe and detect trace levels of carbon dioxide in the 2051-nm spectral region where its beam properties, tunability, narrow linewidth, and stability all coalesce to permit this application. This work indicates this transmitter can serve as a robust source for sensing carbon dioxide and other trace gasses in the short-wave infrared spectral region and should therefore play an important role in future applications.

©2011 Optical Society of America

OCIS codes: (190.4970) Parametric amplifiers and oscillators; (190.4380) Nonlinear optics, four-wave mixing; (190.4370) Nonlinear optics, fiber.

References and links

1. M. Ebrahim-Zadeh, and I. T. Sorokina, eds., *Mid-Infrared Coherent Sources and Applications* (Springer, 2007).
2. C. Weitkamp, ed., *Lidar: Range-Resolved Optical Remote Sensing of the Atmosphere* (Springer, 2005).
3. M. Raybaut, T. Schmid, A. Godard, A. K. Mohamed, M. Lefebvre, F. Marnas, P. Flamant, A. Bohman, P. Geiser, and P. Kaspersen, "High-energy single-longitudinal mode nearly diffraction-limited optical parametric source with 3 MHz frequency stability for CO₂ DIAL," *Opt. Lett.* **34**(13), 2069–2071 (2009).
4. G. J. Koch, B. W. Barnes, M. Petros, J. Y. Beyon, F. Amzajerjian, J. Yu, R. E. Davis, S. Ismail, S. Vay, M. J. Kavaya, and U. N. Singh, "Coherent differential absorption lidar measurements of CO₂," *Appl. Opt.* **43**(26), 5092–5099 (2004).
5. A. Henderson, and R. Stafford, "Low threshold, singly-resonant CW OPO pumped by an all-fiber pump source," *Opt. Express* **14**(2), 767–772 (2006).
6. T. F. Refaat, M. N. Abedin, G. J. Koch, S. Ismail, and U. Singh, "Infrared Detectors Characterization for CO₂ DIAL Measurement," *Proc. SPIE* **5154** Lidar Remote Sensing for Environmental Monitoring IV, 65–73 (2003).
7. P. C. Becker, N. A. Olsson, and J. R. Simpson, *Erbium-Doped Fiber Amplifiers: Fundamentals and Technology* (Academic Press, 1999).
8. N. K. Dutta, and Q. Wang, *Semiconductor Optical Amplifiers* (World Scientific, 2006).
9. E. Nisbet, and R. Weiss, "Atmospheric science: top-down versus bottom-up," *Science* **328**(5983), 1241–1243 (2010).
10. B. B. Stephens, K. R. Gurney, P. P. Tans, C. Sweeney, W. Peters, L. Bruhwiler, P. Ciais, M. Ramonet, P. Bousquet, T. Nakazawa, S. Aoki, T. Machida, G. Inoue, N. Vinnichenko, J. Lloyd, A. Jordan, M. Heimann, O. Shibistova, R. L. Langenfelds, L. P. Steele, R. J. Francey, and A. S. Denning, "Weak northern and strong tropical land carbon uptake from vertical profiles of atmospheric CO₂," *Science* **316**(5832), 1732–1735 (2007).
11. S. L. Lewis, G. Lopez-Gonzalez, B. Sonké, K. Affum-Baffoe, T. R. Baker, L. O. Ojo, O. L. Phillips, J. M. Reitsma, L. White, J. A. Comiskey, M. N. Djuikouo K. C. E. N. Ewango, T. R. Feldpausch, A. C. Hamilton, M. Gloor, T. Hart, A. Hladik, J. Lloyd, J. C. Lovett, J.-R. Makana, Y. Malhi, F. M. Mbago, H. J. Ndangalasi, J. Peacock, K. S.-H. Peh, D. Sheil, T. Sunderland, M. D. Swaine, J. Taplin, D. Taylor, S. C. Thomas, R. Votere, and H. Wöll, "Increasing carbon storage in intact African tropical forests," *Nature* **457**(7232), 1003–1006 (2009).
12. S. Piao, J. Fang, P. Ciais, P. Peylin, Y. Huang, S. Sitch, and T. Wang, "The carbon balance of terrestrial ecosystems in China," *Nature* **458**(7241), 1009–1013 (2009).
13. W. Peters, A. R. Jacobson, C. Sweeney, A. E. Andrews, T. J. Conway, K. Masarie, J. B. Miller, L. M. P. Bruhwiler, G. Pétron, A. I. Hirsch, D. E. J. Worthy, G. R. van der Werf, J. T. Randerson, P. O. Wennberg, M. C. Krol, and P. P. Tans, "An atmospheric perspective on North American carbon dioxide exchange: CarbonTracker," *Proc. Natl. Acad. Sci. U.S.A.* **104**(48), 18925–18930 (2007).

#140287 - \$15.00 USD Received 3 Jan 2011; revised 16 Mar 2011; accepted 22 Mar 2011; published 14 Apr 2011
(C) 2011 OSA 25 April 2011 / Vol. 19, No. 9 / OPTICS EXPRESS 8173

14. G. R. van der Werf, D. C. Morton, R. S. DeFries, J. G. J. Olivier, P. S. Kasibhatla, R. B. Jackson, G. J. Collatz, and J. T. Randerson, "CO₂ emissions from forest loss," *Nat. Geosci.* **2**(11), 737–738 (2009).
15. M. O. Andreae, and P. Merlet, "Emission of trace gases and aerosols from biomass burning," *Global Biogeochem. Cycles* **15**(4), 955–966 (2001).
16. A. Lavrov, A. B. Utkin, R. Vilar, and A. Fernandes, "Applications of lidar in ultraviolet, visible, and infrared ranges for early forest fire detection," *Appl. Phys. B* **76**(1), 87–95 (2003).
17. J. S. Gregg, L. M. Losey, R. J. Andres, T. J. Blasing, and G. Marland, "The Temporal and Spatial Distribution of Carbon Dioxide Emissions from Fossil-Fuel Use in North America," *J. Appl. Meteorol. Climatol.* **48**(12), 2528–2542 (2009).
18. R. T. Menzies, and D. M. Tratt, "Differential laser absorption spectrometry for global profiling of tropospheric carbon dioxide: selection of optimum sounding frequencies for high-precision measurements," *Appl. Opt.* **42**(33), 6569–6577 (2003).
19. L. S. Rothman, I. E. Gordon, A. Barbe, D. C. Benner, P. F. Bernath, M. Birk, V. Boudon, L. R. Brown, A. Campargue, and J.-P. Champion, "The HITRAN 2008 molecular spectroscopic database," *J. Quant. Spectrosc. Radiat. Transf.* **110**(9-10), 533–572 (2009).
20. J. Boggio, S. Moro, B. P.-P. Kuo, N. Alic, B. Stossel, and S. Radic, "Tunable Parametric All-Fiber Short-Wavelength IR Transmitter," *J. Lightwave Technol.* **28**(4), 443–447 (2010).
21. B. P.-P. Kuo, A. O. J. Wiberg, E. Myslivets, D. Blessing, N. Alic, and S. Radic, "Widely-Tunable, Multi-Wavelength Short Wave Infrared Light Source based on Fiber Optical Parametric Oscillator," in *Proc. OFC/NFOEC 2010, San Diego, CA, paper OThA5* (2010).
22. E. Myslivets, N. Alic, and S. Radic, "Spatially Resolved Measurement in Waveguides With Arbitrary Chromatic Dispersion," *IEEE Photon. Technol. Lett.* **20**(21), 1793–1795 (2008).
23. J. M. Chavez Boggio, S. Zlatanovic, F. Gholami, J. M. Aparicio, S. Moro, K. Balch, N. Alic, and S. Radic, "Short wavelength infrared frequency conversion in ultra-compact fiber device," *Opt. Express* **18**(2), 439–445 (2010).
24. R. Jiang, R. E. Saperstein, N. Alic, M. Nezhad, C. J. McKinstrie, J. E. Ford, Y. Fainman, and S. Radic, "Continuous-Wave Band Translation Between the Near-Infrared and Visible Spectral Ranges," *J. Lightwave Technol.* **25**(1), 58–66 (2007).
25. R. Jiang, C.-S. Bres, N. Alic, E. Myslivets, and S. Radic, "Translation of Gbps Phase-Modulated Optical Signal From Near-Infrared to Visible Band," *J. Lightwave Technol.* **26**(1), 131–137 (2008).
26. C. J. McKinstrie, M. Yu, M. G. Raymer, and S. Radic, "Quantum noise properties of parametric processes," *Opt. Express* **13**(13), 4986–5012 (2005).
27. S. Moro, A. Peric, N. Alic, C. J. McKinstrie, and S. Radic, "Experimental Demonstration of a Low-Noise-Figure Phase-Insensitive Parametric Amplifier," *IEEE Photonics Society 2010 Annual Meeting, Denver, CO, paper WN3* (2010).
28. A. Boskovic, S. V. Chernikov, J. R. Taylor, L. Gruner-Nielsen, and O. A. Levring, "Direct continuous-wave measurement of n_2 in various types of telecommunication fiber at 1.55 μm ," *Opt. Lett.* **21**(24), 1966–1968 (1996).
29. F. Gholami, J. M. Chavez Boggio, S. Moro, N. Alic, and S. Radic, "Measurement of ultra-low fourth order dispersion coefficient in nonlinear fiber by distant low-power FWM," *IEEE Photonics Society Summer Topical Meeting, paper WC1.1, Playa Del Carmen, Mexico* (2010).
30. M. E. Marhic, K. K.-Y. Wong, and L. G. Kazovsky, "Wide-Band Tuning of the Gain Spectra of One-Pump Fiber Optical Parametric Amplifiers," *IEEE J. Sel. Top. Quantum Electron.* **10**(5), 1133–1141 (2004).
31. M. Hirano, T. Nakanishi, T. Okuno, and M. Onishi, "Silica-Based Highly Nonlinear Fibers and Their Application," *IEEE J. Sel. Top. Quantum Electron.* **15**(1), 103–113 (2009).
32. V. A. Kovalev, and W. E. Eichinger, *Elastic Lidar: Theory, Practice, and Analysis Methods* (Wiley, 2004), Ch. 7.
33. S. Kameyama, T. Ando, K. Asaka, Y. Hirano, and S. Wadaka, "Compact all-fiber pulsed coherent Doppler lidar system for wind sensing," *Appl. Opt.* **46**(11), 1953–1962 (2007).

1. Introduction

Over the short-wave infrared (SWIR) spectrum, which is typically defined as spanning from 1700 to 2500 nm, a variety of molecular gases and environmental pollutants exhibit strong well-defined absorption features [1]. To detect their unique "fingerprints" requires remote sensing in the SWIR band via a light detection and ranging (LIDAR) technique which must itself rely on high-power, high-frequency-fidelity, tunable laser sources in conjunction with low-noise photodetectors [2]. The state-of-the-art SWIR sources that have been utilized in LIDAR systems to date are custom-made, crystal-based, optical parametric oscillators (OPOs), providing multiple Watts of output power and typical linewidths of several MHz [1,3,4]. To their credit, these OPOs allow broadband tunability (hundreds of nanometers); however, their mode-hop-free tuning range is limited to approximately 100 GHz (order of 1 nm), which precludes their use in sensitive spectroscopy applications [5]. Another practical limitation to the widespread use of traditional OPOs for this application is their construction. OPOs rely on free-space optical elements and as such they are highly sensitive to thermal and

vibration perturbations; their performance when fielded is depreciated over that which can be demonstrated in a laboratory environment. Furthermore, SWIR-based LIDAR is not only plagued by these source-specific issues but is also impaired by a lack of sensitive, high-bandwidth photodetectors. The most promising detector technology in the SWIR band has been shown to be extended-band InGaAs, still the performance of these devices is frustrated by high thermal and dark current noise due to the reduced semiconductor bandgap at these wavelengths and the high impurity and defect concentrations [6].

Sources and detectors available in the SWIR band contrast sharply with their near-infrared (NIR) (800-1700 nm) counterparts which have benefited from years of intense commercial development predominantly driven by the optical telecommunications industry. As a result, mode-hop-free, widely-tunable, narrow-linewidth NIR sources are readily available and relatively inexpensive. Furthermore, NIR InGaAs(P) photoreceivers have significantly lower dark current and thermal noise than their SWIR equivalents. The photodetection sensitivity in the NIR band can also be improved by several orders of magnitude through optical pre-amplification. Here the combination of rare-earth doped fiber amplifiers (Erbium- and Ytterbium-doped fiber amplifiers) and semiconductor optical amplifiers (SOAs) provides for more than 30 dB of optical gain over the entire NIR spectrum with routinely reproducible low noise figures in 3-5 dB range [7,8].

In this work, a widely-tunable, cavity-less parametric transmitter operating in the SWIR wavelength range was constructed and used to detect the presence of carbon dioxide. An important aspect of this transmitter, one that cannot be overemphasized, is that it is constructed entirely of NIR components and, as a consequence, benefits from the high-quality performance and low cost of these constituent elements. The ability to remotely sense carbon dioxide is not only a good proof-of-principle experiment but is of critical importance in climate change studies, long-term weather forecasting, early forest fire detection, and global fossil-fuel combustion monitoring [9–17]. We specifically chose to probe the R30 absorption line of CO₂, centered at 2050.967 nm, because of the high contrast it exhibits with respect to problematic water vapor and its inherently low temperature sensitivity [18]. The results obtained in this work are in excellent agreement with absorption data obtained from the High-resolution TRANsmission molecular absorption database (HITRAN2008) [19].

2. Parametric SWIR Transmitter: Experimental Results and Discussion

Single-pass fiber-optic parametric amplifiers/converters (FOPA/Cs) have recently been identified as a practical platform for bridging the gap between the spectrally important SWIR band, where few components exist, and the technologically developed NIR band [20,21]. On the transmitter end, the FOPC offers efficient wide band NIR-to-SWIR conversion by means of phase-matched four-wave mixing (FWM) in dispersion-engineered highly-nonlinear fiber (HNLF). In this process two NIR pump photons are annihilated while the existing NIR signal wave is amplified and a newly-generated, so-called ‘idler,’ wave is created in the SWIR band. The transmitter’s all-fiber construction allows for long nonlinear interaction lengths which results in high conversion gains. The ability to optimize the parametric gain spectrum and its magnitude is critically dependent on the dispersive properties of the HNLF and therefore one’s ability to accurately measure and subsequently minimize the HNLF’s local dispersion fluctuations [22]. The high-index-contrast of the transmitter’s HNLF, which confers increased nonlinearity and tailored dispersion, also yields the fiber highly resilient to macrobending, allowing for ultracompact packaging of the nonlinear mixer [23]. The FWM interaction also allows any amplitude or phase coding imparted on the signal wave to be converted to the newly-generated idler [24,25]. On the receiving end of a system, a FOPA can also play a critical role by enabling the creation of an optically pre-amplified receiver anywhere in the SWIR band. A well-designed FOPA is limited only by a 3-dB noise figure which is theoretically associated with phase-insensitive amplifiers [26]. Therefore, these amplifiers outperform their technologically-mature inverted-population counterparts (EDFAs and SOAs) at low input signal power levels [27]. Because the FOPA/C described in this work rely on a traveling-wave construction (i.e. they are cavity-less), they circumvent all the impairments

associated with conventional OPO designs including cavity stability, limited mode-hop-free tuning range, and tuning speed.

The SWIR parametric transmitter used in this work is depicted at the top of Fig. 1. The pump source was a tunable external-cavity laser (ECL), which was amplitude modulated to produce 500-ps pulses with a 0.05% duty cycle to avoid saturation effects in the EDFAs. The modulated pump was subsequently amplified and excess amplified spontaneous emission (ASE) noise was rejected using a pair of band-pass optical filters. Another ECL, tunable from 1260 to 1360nm, was chosen as the signal source to enable precision tuning of the signal and, as a consequence, idler wavelengths. The amplified pump pulse and continuous-wave signal seed were combined and sent into a 7-m-long HNLF with a nonlinear coefficient $15 \text{ W}^{-1}\text{km}^{-1}$ measured using the method reported in [28]. The HNLF's zero-dispersion wavelength (ZDW) of 1583.0 nm and the dispersion slope of $0.027 \text{ ps/nm}^2\text{-km}$ were measured using a commercial lightwave analyzer (Advantest Q7750), while the fourth-order dispersion coefficient was measured at $1.4 \times 10^{-5} \text{ ps}^4/\text{km}$ via the method reported in [29]. The HNLF coil used in this work was chosen because it provided the lowest available positive fourth-order dispersion. This parameter negatively affects phase-matching when the signal-to-idler's spectral separation becomes large and we therefore seek to minimize its contribution in order to permit broadband parametric gain synthesis.

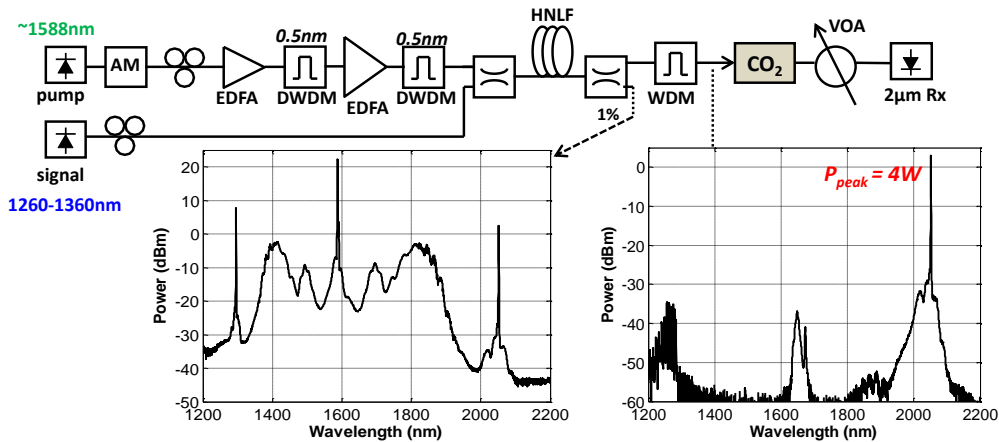


Fig. 1. Experimental setup depicting (top) the parametric SWIR transmitter; (bottom left) the optical spectrum following NIR-to-SWIR conversion in HNLF; (bottom right) the optical spectrum following rejection of pump, signal, and excess amplified quantum noise; Acronyms: AM – amplitude modulator, EDFA – Erbium doped fiber amplifier, DWDM – dense wavelength division multiplexer, VOA – variable optical attenuator, Rx – optical receiver.

The left inset in Fig. 1 depicts the optical spectrum following parametric amplification and conversion in the HNLF. The pump wavelength was set to 1587.9 nm and the signal wavelength to 1295.4 nm, resulting in the 2051.0-nm idler wave at the output of the FOPC. The broadband amplified quantum noise (AQN) is present in approximately a 600-nm bandwidth around the optical pump, due to the high degree of phase matching that exists at these wavelengths. The broadband AQN can be completely done away with by employing HNLFs with negative fourth-order dispersion coefficient [30]. However, such nonlinear fibers are characterized by increased dispersion slopes and therefore increased sensitivity of phase-matching to local ZDW fluctuations [31]. For this reason, efficient broadband conversion (beyond 2 μm) in these devices has not yet been reported to the best of the authors' knowledge. The pump, signal, and excess AQN were filtered out using several wavelength-division multiplexers (WDMs) and the resulting parametric SWIR source spectrum is shown in the bottom right inset of Fig. 1.

The measured conversion gain spectrum shown in Fig. 2(a) for several different pump wavelength positions indicates the spectral tunability available to this source while

simultaneously hinting that the spectral stability of the pump is critical for this application. The conversion gain is defined as the ratio of the output idler power to the input signal power. The pump power was set to 54.6 dBm and the wavelength detuned over approximately 4 nm in the L band, resulting in a conversion gain peak shift across a 150-nm bandwidth. The conversion gain peak can therefore be positioned arbitrarily in the SWIR band via a small detuning of the pump wavelength. In order to place the FWM peak at the R30 line of CO₂, the pump wavelength was detuned to 1587.9 nm which produced the conversion gain spectrum shown in Fig. 2(b). The peak conversion gain of 31 dB resulted in 4 W of measured idler peak power at the wavelength of 2051 nm as previously indicated in Fig. 1 (bottom right).

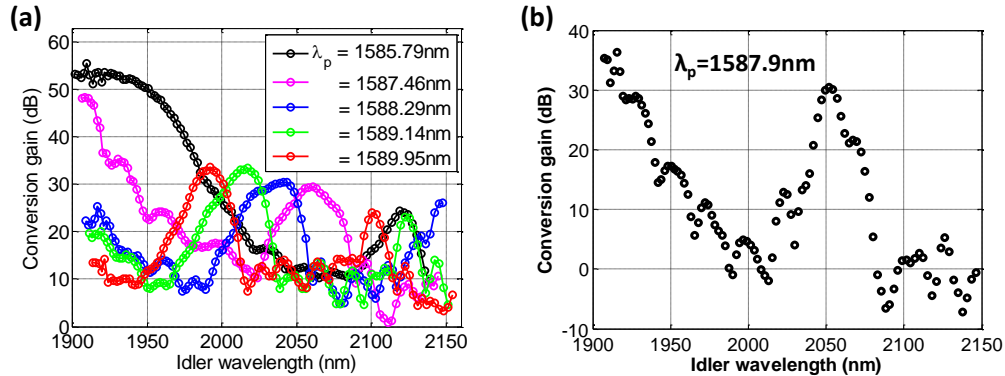


Fig. 2. (a) Measured conversion gain spectra for several different pump wavelength positions; (b) Measured conversion gain spectrum with pump wavelength optimized for peak conversion gain at 2051 nm.

Following the rejection of pump, signal, and excess AQN by the WDMs, the idler pulse was sent through a 24-cm CO₂ cell held at a constant pressure of 600 Torr. The idler pulse was subsequently attenuated using a variable optical attenuator to milliwatt power levels acceptable for a commercially available 5-GHz bandwidth, 2- μ m, extended-band InGaAs p-i-n photodetector (EOT, Inc.). By subtly changing the pump wavelength the idler was precisely tuned to the four different positions shown in Fig. 3(a). One of the wavelength positions (color coded blue) was purposely centered off-line, while the other three were exactly positioned at three different absorption peaks. The absorption spectrum of CO₂, obtained from the HITRAN2008 database is included in Fig. 3(b) to show the relative strengths of the different absorption peaks. The received idler pulses corresponding to the four different wavelength positions were displayed on an electrical equivalent-time scope and are shown in Fig. 3(c). As expected, the longer wavelength on-line idlers were attenuated more strongly by the CO₂ cell. The slope of the on-line idlers is due to slight chirping of the pulse in the parametric SWIR transmitter setup. The SWIR idler's electrical SNR was measured to be in excess of 30 dB over the entire tuning range.

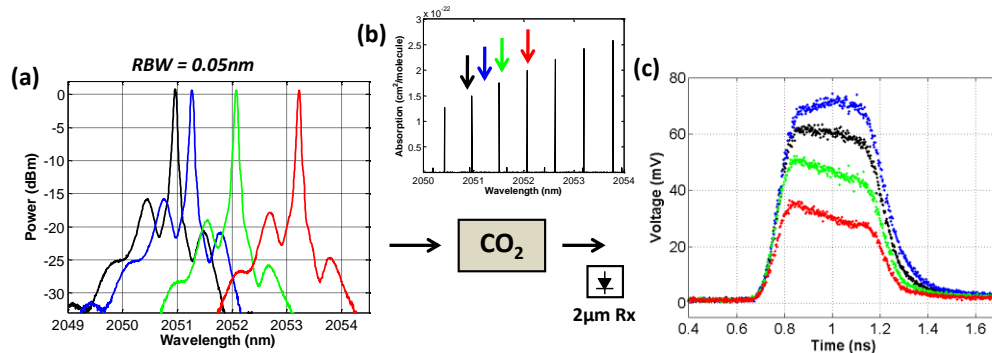


Fig. 3. (a) Measured idler optical spectra at four different positions; (b) CO₂ absorption data obtained from HITRAN2008 database; (c) Measured idler pulses corresponding to the four different idler wavelengths shown in (a).

At this point we wish to emphasize an important benefit of using parametric SWIR transmitters which cannot be matched by conventional devices operating in the SWIR band. While the pump pulse is in its “off” state, the only photons that exist at the idler wavelength are due to zero-point vacuum field fluctuations. As a result, the SWIR idler pulse possesses a *vacuum-limited extinction ratio*. Poor pulse extinction ratios result in so-called ghost LIDAR returns which severely limit the sensing range of the system [32]. To mitigate this problem, some commercial all-fiber LIDAR technologies employ a cascade of acousto-optic modulators in order to achieve extinction ratios of more than 100 dB, which allows for an operation range of approximately 1 km [33]. Keeping in mind that the technical requirements placed on longer range LIDAR systems grow with the square of the distance from the sensed target, the parametric conversion platform offers an inherent solution as the sensing system is never extinction-ratio-limited.

3. Conclusion

In this work, carbon-dioxide trace detection has been demonstrated for the first time using a continuously tunable parametric SWIR transmitter. Although this device has obvious implications for DIAL-type systems, we found it had a sufficient margin to operate even without relying on a differential-detection scheme. Clearly, such a scheme can be used to further improve its performance in the future.

The transmitter utilizes a dispersion-engineered highly-nonlinear fiber platform for efficient wavelength conversion from NIR to SWIR band while using conventional NIR components.

By precisely controlling the pump wavelength position, the conversion gain spectrum was accurately tuned to probe a number of absorption lines of carbon dioxide in this proof-of-concept demonstration. Overall we feel this platform offers a practical way to leverage the benefits of advanced NIR technology for sensing and spectroscopy in the poorly-developed SWIR band. Moreover, the all-fiber design represents a significant advancement in terms of portability, stability, and cost when compared to existing SWIR technologies.

Acknowledgements

This material is based on research sponsored by the DARPA under agreement number FA8650-08-1-7819 Parametric Optical Processes and Systems. N. G. Usechak is supported through AFOSR LRIR 09RY04COR. Part of this work was also supported by Lockheed Martin Corporation. The authors would like to thank Sumitomo Electric Ltd. for providing the nonlinear fiber.